Modeling of $^{12}C^{16}O_2$ line intensities in the region from 4377 to 5703 cm^{-1}

S.A. Tashkun

Institute of Atmospheric Optics,
Siberian Branch of the Russian Academy of Sciences, Tomsk

Received May 20, 2003

The results of global fitting of effective dipole moment parameters to measured line intensities of the principal isotopic species $^{12}C^{16}O_2$ borrowed from the literature are presented. Using a model with 14 parameters, we succeeded in reproducing the intensities of almost 900 lines belonging to 16 bands with the RMS error = 5.6%. With the help of the model fitted, a line list for temperature T = 296 K and intensity cut-off $I_{cut} = 10^{-27}$ $cm^{-1}/(molecule\ cm^{-2})$ was generated. The line list will be a part of the future atmospheric version of the CDSD databank. The comparison of the line list with the HITRAN CO_2 data is given as well.

Introduction

Knowledge of radiative properties of the CO_2 molecule in the 2-μm region is important not only for atmospheric applications, but also for modeling the emission spectrum of the Venus nightside atmosphere,[1] as well as for the development of high-temperature diode-laser sensors.[2] Global fits of positions[3] and intensities[4] of $^{12}C^{16}O_2$ rotational-vibrational lines were made in 1998–1999 based on the effective operator approach. In Ref. 4 the 2-μm region was presented by 342 line intensities borrowed from Refs. 5–9 and belonging to four bands. Using a model of effective dipole moment operator with nine fitted parameters, we obtained the RMS deviation of 7.8%.

In recent years line intensities have been recorded within some new bands falling within the studied region.[2,10–14] Besides, Dr. Wattson[15] pointed to the fact that the line intensities for the 31103–00001 band included in HITRAN have also been measured. Thus, a total, intensities of more than 500 lines belonging to twelve new bands are now available. Comparison of the measured intensity values with those from the HITRAN database[16] is illustrated in Fig. 1.

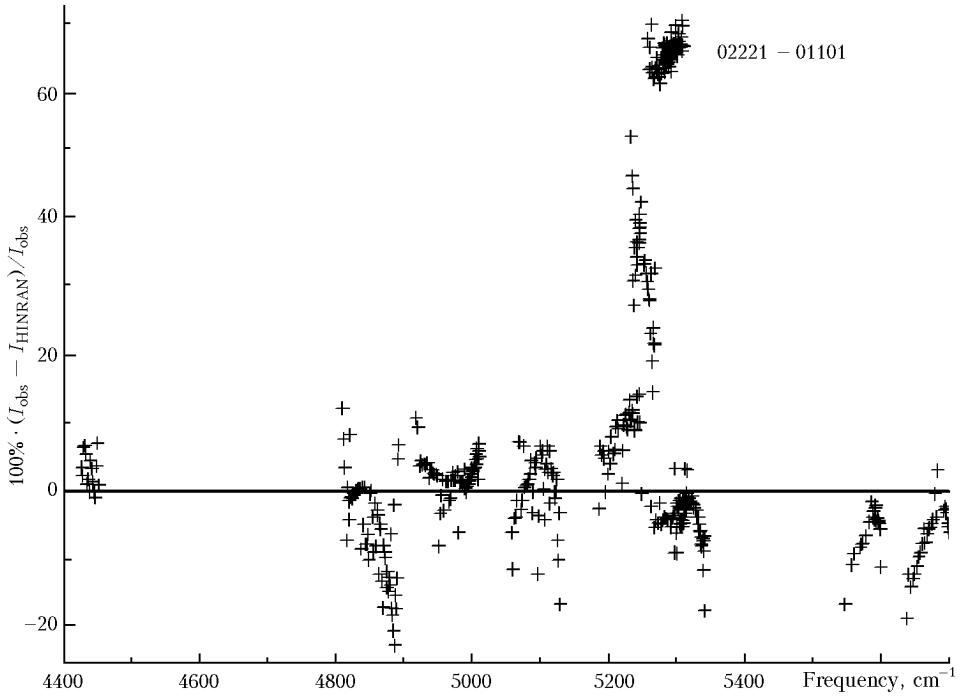

Fig. 1. Comparison of the observed intensities with those from HITRAN.

0235-6880/03/08 621-05 $02.00

One can see significant discrepancies between measurements and the HITRAN data. Thus, for the 02221–01101 band the mean deviation by the $100\% \cdot (I_{obs} - I_{HITRAN})/I_{obs}$ criterion is ~ 70%. If we compare line intensities directly, the difference may achieve several times. As an example, consider the $R17$ line of this band, which is positioned nearby 5303.47 cm^{-1}. Its measured intensity is $0.391 \cdot 10^{-25}$ $cm^{-1}/(mol. \cdot cm^{-2})$, while in the HITRAN database it is equal to $0.132 \cdot 10^{-25}$ $cm^{-1}/(mol. \cdot cm^{-2})$. Some of the bands measured, for example, 10021–01101 are even absent in HITRAN.

New fitting is very urgent because of a large number of new measured data and wide discrepancies between measured line intensities and those in the HITRAN database. The new fitted parameters of the dipole moment operator will be used for generation of a new version of the CDSD databank (Carbon Dioxide Spectroscopic Databank) for atmospheric and high-temperature[17] applications.

Experimental data

Experimental line intensities from Refs. 2, 5–14, and 16 were compiled in a single data file. These data are summarized in Table 1, which presents the rovibrational bands, the maximum value of the rotational quantum number J for each band, the number of lines, the band center, the estimated vibrational intensity, and the corresponding reference.

Table 1. Observed data involved in the fitting procedure

Band	J_{max}	Number of lines	ν_0*	S_V^{0}**	Ref.
20012 00001	60	194	4978	347.5	2, 5, 7, 8, 12
20011 00001	60	91	5100	109.0	5, 12
20013 00001	59	143	4854	78.1	5, 6, 12
31104 00001	60	51	4416	0.00024	9
32203 01101	36	32	4578	–	10
40004 01101	44	12	4530	–	10
40002 01101	16	1	4808	–	11
21113 01101	16	1	4808	–	11
01121 00001	60	84	5315	0.476	11, 14
00031 10002	50	37	5687	0.0068	13
00031 10001	51	29	5584	0.0063	13
30011 10002	43	34	5218	0.0228	14
10022 01101	40	37	5248	0.0136	14
02221 01101	38	88	5291	0.0360	14
10021 01101	34	21	5349	0.0051	14
31103 00001	60	68	4591	0.00289	16

* band center (cm^{-1}); ** vibrational band intensity $(cm^{-1}/(mol. \cdot cm^{-2}) \cdot 10^{-22})$ at T = 296 K.

Unfortunately, most of the experimental studies do not give information on the measurement accuracy. In the cases that the accuracy is given in the references, its values were used in the fitting. In other cases, we used the values taken based on the experimental instrumentation used and the period of spectrum recording. It is clear that these values are subjective to some extent. The measurement accuracy used in the fitting procedure is given in the fourth column of Table 2.

Table 2. Band-ordered fit results

Band	Branch	J_{max}	Number of lines	RMS, %	MR, 5
00031–10001	P	35	8	5.1	–2.8
00031–10001	R	39	14	3.9	0.3
00031–10002	P	51	23	2.7	–0.1
00031–10002	R	37	14	1.4	0.5
01121–00001	P	61	24	6.9	–5.0
01121–00001	Q	61	29	2.5	1.0
01121–00001	R	57	28	5.4	5.1
02221–01101	P	36	24	8.3	4.9
02221–01101	Q	40	31	3.0	–0.5
02221–01101	R	38	31	7.0	–3.8
10021–01101	P	32	9	9.0	7.9
10021–01101	Q	35	12	6.6	–2.9
10022–01101	P	18	6	13.7	8.9
10022–01101	Q	41	14	4.5	–1.3
10022–01101	R	38	15	7.6	–1.5
20011–00001	P	47	41	4.8	1.2
20011–00001	R	45	39	4.2	1.5
20012–00001	P	61	91	3.8	–1.1
20012–00001	R	59	93	2.8	–0.4
20013–00001	P	51	61	4.8	–1.8
20013–00001	R	59	71	6.0	–1.7
21113–01101	R	16	1	8.0	–8.0
30011–10002	P	37	15	5.0	–3.4
30011–10002	R	43	19	2.9	–0.9
31104–00001	P	55	22	10.2	0.2
31104–00001	R	61	29	6.3	1.0
31103–00001	P	57	22	4.1	1.0
31103–00001	Q	35	16	1.0	0.8
31103–00001	R	61	30	3.6	0.0
32203–01101	P	38	13	10.4	–2.7
32203–01101	R	33	17	12.4	–7.1
40002–01101	R	16	1	0.3	–0.3
40004–01101	R	44	10	10.3	9.3

Fit of line intensities

The intensity $S_{b \leftarrow a}(T)$ [in $cm^{-1}/(mol. \cdot cm^{-2})$] of a rovibrational transition $b \leftarrow a$ under LTE (local thermodynamic equilibrium) conditions is determined by the known equation:

$$S_{b \leftarrow a}(T) = \frac{8\pi^3}{3hc} C\sigma_{b \leftarrow a} \frac{\exp(-hcE_a/kT)}{Q(T)} \times$$

$$\times (1 - \exp(-hc\sigma_{b \leftarrow a}/kT)) W_{b \leftarrow a}, \qquad (1)$$

where T is temperature; C is the abundance of a given isotopic species; $\sigma_{b \leftarrow a}$ is the frequency of transition from the lower state a into the upper state b; E_a is the lower-state energy; k is the Boltzmann constant; $Q(T)$ is the partition function; c is the speed of light; h is the Planck's constant; $W_{b \leftarrow a}$ is the probability of transition from the state a to the state b.

In this paper, we use the phenomenological model of the effective dipole moment operator. The operator is a linear combination of symmetry-allowed elementary vibrational and rotational basis operators written up to a given order of the perturbation theory. The coefficients of this linear combination are usually declared variable parameters. This model leads to a serial approach, in which all vibrational

bands break into non-overlapping series. Each series is determined by the difference

$$\Delta P = 2(\nu_1' - \nu_1) + (\nu_2' - \nu_2) + 3(\nu_3' - \nu_3),$$

where ν_1', ν_2', ν_3' and ν_1, ν_2, ν_3 are the indices of normal modes of the upper and lower states of a band. All the bands considered in this paper have $\Delta P = 7$. Within the approach selected, the equation for the probability of the transition $W_{b \leftarrow a} = W_{N'J'\varepsilon' \leftarrow NJ\varepsilon}$ between the states identified by the vibrational index N, the rotational quantum number J, and the parity $\varepsilon = \pm 1$ has the following form[4]:

$$W_{N'J'\varepsilon' \leftarrow NJ\varepsilon} = (2J+1) \times$$

$$\times \left| \sum_{\nu_1 \nu_2 l_2 \nu_3} \sum_{2\Delta\nu_1 + \Delta\nu_2 + 3\Delta\nu_3 = 7} \sum_{\Delta l_2 = 0, \pm 1, \pm 2, \ldots} C_{N,\varepsilon}^{J,\nu_1,\nu_2,l_2,\nu_3} \times \right.$$

$$\times C_{N',\varepsilon'}^{J',\nu_1+\Delta\nu_1,\nu_2+\Delta\nu_2,l_2+\Delta l_2,\nu_3+\Delta\nu_3} M_{\Delta\nu_1,\Delta\nu_2,\Delta\nu_3}^{|\Delta l_2|} \times$$

$$\times \sqrt{f_{\Delta\nu_1,\Delta\nu_2,\Delta\nu_3}^{\Delta l_2}(\nu_1,\nu_2,l_2,\nu_3)(1 + \delta_{l_2,0} + \delta_{l_2',0} - 2\delta_{l_2,0}\delta_{l_2',0})} \times$$

$$\times (1, \Delta l_2, J, l_2 \mid J', l_2 + \Delta l_2)[1 +$$

$$\left. + \sum_{i=1}^{3} \kappa_i^{\Delta\nu_1,\Delta\nu_2,\Delta\nu_3} \nu_i + F_{\Delta l_2}^{\Delta\nu_1,\Delta\nu_2,\Delta\nu_3}(l_2, J)] \right|^2. \qquad (2)$$

In Eq. (2) $C_{N,\varepsilon}^{J,\nu_1,\nu_2,l_2,\nu_3}$ are the mixing coefficients determining expansion of the eigenfunctions of the effective lower-state Hamiltonian in terms of the basis functions

$$\Psi_{NJM\varepsilon}^{\text{eff}} = \sum_{\nu_1 \nu_2 l_2 \nu_3} C_{N,\varepsilon}^{J,\nu_1,\nu_2,l_2,\nu_3} \mid \nu_1, \nu_2, \mid l_2 \mid, \nu_3, J, M, \varepsilon >,$$

where M is the magnetic quantum number. The mixing coefficients of the upper state $C_{N',\varepsilon'}^{J',\nu_1,\nu_2,l_2',\nu_3}$ can be found in the similar way. In fact, the mixing coefficients are components of the normalized eigenvectors corresponding to the appropriate energy levels of the model of effective Hamiltonian used for calculation of transition probabilities. In this paper, we took the model obtained from global fitting of line positions and reported in Ref. 3 as a model of effective Hamiltonian.

The values of the function $f_{\Delta\nu_1,\Delta\nu_2,\Delta\nu_3}^{\Delta l_2}(\nu_1,\nu_2,l_2,\nu_3)$ for small $\Delta\nu_1$, $\Delta\nu_2$ and $\Delta\nu_3$ can be found in Ref. 18; $(1, \Delta l_2, J, l_2 \mid J', l_2 + \Delta l_2)$ is the Clebsch–Gordon coefficient. The function $F_{\Delta l_2}^{\Delta\nu_1,\Delta\nu_2,\Delta\nu_3}(l_2, J)$ depends on the type of the band and the branch. For parallel bands ($\Delta l_2 = 0$) it has the form

$$F_0^{\Delta\nu_1,\Delta\nu_2,\Delta\nu_3}(l_2, J) = b_J^{\Delta\nu_1,\Delta\nu_2,\Delta\nu_3} m +$$

$$+ d_J^{\Delta\nu_1,\Delta\nu_2,\Delta\nu_3}[J(J+1) + m - l_2^2], \qquad (3)$$

where $m = -J$, 0, $J+1$ for the P-, Q-, and R-branches, respectively. For the perpendicular ($\Delta l_2 \neq 0$) band, the values of this function depend on the branch. It can be presented as

$$F_{\Delta l_2}^{\Delta\nu_1,\Delta\nu_2,\Delta\nu_3}(l_2, J) = -\frac{1}{2} b_J^{\Delta\nu_1,\Delta\nu_2,\Delta\nu_3}(2 l_2 \Delta l_2 + 1) +$$

$$+ d_{JQ}^{\Delta\nu_1,\Delta\nu_2,\Delta\nu_3} J(J+1) - l_2^2 - \Delta l_2 (l_2 + \frac{\Delta l_2}{2}) \qquad (4)$$

for the Q-branch and as

$$F_{\Delta l_2}^{\Delta\nu_1,\Delta\nu_2,\Delta\nu_3}(l_2, J) = -\frac{1}{4}(d_{JQ}^{\Delta\nu_1,\Delta\nu_2,\Delta\nu_3} - d_J^{\Delta\nu_1,\Delta\nu_2,\Delta\nu_3}) +$$

$$+ \frac{1}{2}(b_J^{\Delta\nu_1,\Delta\nu_2,\Delta\nu_3} + d_{JQ}^{\Delta\nu_1,\Delta\nu_2,\Delta\nu_3})(2 l_2 \Delta l_2 + 1) +$$

$$+ d_{JQ}^{\Delta\nu_1,\Delta\nu_2,\Delta\nu_3} l_2^2 + b_J^{\Delta\nu_1,\Delta\nu_2,\Delta\nu_3} m + d_J^{\Delta\nu_1,\Delta\nu_2,\Delta\nu_3} m^2 +$$

$$+ (d_{JQ}^{\Delta\nu_1,\Delta\nu_2,\Delta\nu_3} - d_J^{\Delta\nu_1,\Delta\nu_2,\Delta\nu_3}) m (l_2 \Delta l_2 + \frac{1}{2}) \qquad (5)$$

in the case of the P- and R-branches. The parameters $M_{\Delta\nu_1,\Delta\nu_2,\Delta\nu_3}^{|\Delta l_2|}$, $\kappa_i^{\Delta\nu_1,\Delta\nu_2,\Delta\nu_3}$, $b_J^{\Delta\nu_1,\Delta\nu_2,\Delta\nu_3}$, $d_J^{\Delta\nu_1,\Delta\nu_2,\Delta\nu_3}$, and $d_{JQ}^{\Delta\nu_1,\Delta\nu_2,\Delta\nu_3}$ are variable. Their values are determined from fitting of theoretical intensity values to experimental ones.

The fitting procedure is aimed at minimization of the dimensionless standard deviation χ defined as follows:

$$\chi = \sqrt{\sum_{i=1}^{N_l} \left(\frac{S_i^{\text{obs}} - S_i^{\text{calc}}}{\delta_i} \right)^2 \Big/ (N_l - n)}, \qquad (6)$$

in which S_i^{obs} and S_i^{calc} are, respectively, the observed and calculated intensity of the ith line; $\delta_i = S_i^{\text{obs}} \sigma_i / 100\%$, where σ_i is the measurement uncertainty for the ith line, in %; N_l is the number of lines involved in the fit; n is the number of fitted parameters.

To characterize the quality of fitting in the cases of deficient information about the measurement uncertainty, it is more convenient to use the rms deviation, which is defined as follows:

$$\text{RMS} = \sqrt{\frac{\sum_{i=1}^{N_l} \left(\frac{S_i^{\text{obs}} - S_i^{\text{calc}}}{S_i^{\text{obs}}} \right)^2}{N_l}} \cdot 100\%. \qquad (7)$$

The third statistical characteristic used in this paper for analysis of the fitting results is the mean residue (MR) for a given branch. The MR parameter is defined by the following equation:

$$\text{MR} = \frac{1}{N_{\text{b}}} \sum_{i=1}^{N_{\text{b}}} \left(\frac{S_i^{\text{obs}} - S_i^{\text{calc}}}{S_i^{\text{obs}}} \right) \cdot 100\%, \qquad (8)$$

in which N_{b} is the number of lines in the branch. For an ideally fitted branch, MR is equal to zero. Large positive and negative values of MR indicate that either the calculated values of the line intensities are systematically shifted with respect to the

experimental ones or experimental data include significant errors.

The fit results for different bands are given in Table 2, RMS for each of the used references is given in Table 3, and the fitted parameters of the dipole moment operator along with the standard errors are given in Table 4. It should be noted that to achieve RMS = 5.6%, we had to remove 50 lines statistically identified as spikes from fitting.

Table 3. Reference-ordered fit results

Reference	Number of lines	Number of bands	σ*, %	RMS, %
2	3	1	3	2.5
5	108	3	6	6.2
6	54	1	1–30	5.0
7	55	1	1–5	1.5
8	33	1	7	1.4
9	51	1	10	8.2
10	40	2	10	11.3
11	7	3	10	6.0
12	143	2	1–20	3.8
13	58	2	2–10	3.3
14	252	5	2	6.1
16	68	1	5	3.4

* measurement errors used.

Table 4. Parameters of the effective dipole moment operator

Parameter*	Value	Order of magnitude
$M^0_{2,0,1}$	−0.37516(33)**	10^{-2}
$M^0_{1,2,1}$	0.2746(16)	10^{-3}
$M^0_{0,4,1}$	−0.827(38)	10^{-5}
$M^0_{-1,0,3}$	−0.281(80)	10^{-5}
$M^0_{0,-2,3}$	−0.12540(42)	10^{-3}
$M^1_{3,1,0}$	−0.4553(59)	10^{-5}
$b_J^{3,1,0}$	1.263(14)	10^{-2}
$M^1_{0,1,2}$	−0.7596(11)	10^{-4}
$b_J^{0,1,2}$	0.1529(80)	10^{-2}
$M^1_{1,-1,2}$	−0.1661(25)	10^{-4}
$b_J^{1,-1,2}$	1.75(12)	10^{-1}
$d_J^{1,-1,2}$	−0.82(42)	10^{-3}
$M^1_{1,5,0}$	0.157(28)	10^{-6}
$b_J^{1,5,0}$	3.21(43)	10^{-2}

* parameters M are given in D, and parameter b is dimensionless. ** Uncertainty in parenthesis is one standard deviation in units of the last digit of the parameter value.

Results and discussion

The obtained value of RMS = 5.6% shows that the model of the dipole moment operator used is, on the whole, adequate to the experimental data. Analysis of Table 2 shows also that the widest deviations between measurements and calculations are observed for weak bands. This is quite clear, because weak bands are usually recorded with larger errors than the strong bands. It also follows from Table 3 that for almost all sources of the experimental data the RMS value is close to the measurement accuracy. The only exclusion is Ref. 14, for which the estimated accuracy of 2% is, likely, too optimistic.

Using the parameters obtained, for the region of 4381–5703 cm^{-1}, the temperature of 296 K, and the intensity cut-off of 10^{-27} $cm^{-1}/(mol \cdot cm^{-2})$, we have generated the line list called as CDSD, which will be included in the future atmospheric version of the CDSD databank.[17] Below we compare the CDSD line list with the data for $^{12}C^{16}O_2$ included in the HITRAN databank. In the spectral region studied, HITRAN includes 3542 lines, while CDSD involves 5584 lines. Any line from HITRAN is present in CDSD as well. In addition, CDSD includes 30 bands that are absent from HITRAN. These bands are presented in Table 5.

Table 5. Bands absent from the HITRAN database

Band	Number of lines	Intensity,* $cm^{-1}/(mol \cdot cm^{-2})$
32201–01101	118	$3.817 \cdot 10^{-24}$
31101–00001	72	$2.469 \cdot 10^{-24}$
40001–01101	53	$7.889 \cdot 10^{-25}$
10021–01101	70	$6.511 \cdot 10^{-25}$
24412–04401	56	$1.008 \cdot 10^{-25}$
32212–12201	67	$1.631 \cdot 10^{-25}$
11122–10002	48	$1.391 \cdot 10^{-25}$
32203–01101	54	$1.299 \cdot 10^{-25}$
03321–02201	80	$1.796 \cdot 10^{-25}$
13311–01101	58	$1.033 \cdot 10^{-25}$
13312–01101	56	$9.472 \cdot 10^{-26}$
41101–10001	34	$8.046 \cdot 10^{-26}$
32212–12202	51	$8.110 \cdot 10^{-26}$
01131–11102	51	$8.508 \cdot 10^{-26}$
31111–11102	47	$7.132 \cdot 10^{-26}$
32211–12201	43	$7.259 \cdot 10^{-26}$
40014–20002	32	$6.470 \cdot 10^{-26}$
33302–02201	43	$6.278 \cdot 10^{-26}$
40012–20002	29	$5.663 \cdot 10^{-26}$
40011–20001	28	$5.095 \cdot 10^{-26}$
11121–10001	32	$5.002 \cdot 10^{-26}$
01131–11101	43	$5.947 \cdot 10^{-26}$
32202–01101	26	$4.083 \cdot 10^{-26}$
40013–20003	26	$4.240 \cdot 10^{-26}$
24411–04401	31	$3.728 \cdot 10^{-26}$
40004–01101	17	$3.726 \cdot 10^{-26}$
41102–10002	19	$2.412 \cdot 10^{-26}$
11122–02201	19	$2.030 \cdot 10^{-26}$
22213–10002	7	$7.777 \cdot 10^{-27}$
21122–01111	6	$6.258 \cdot 10^{-27}$

* sum of line intensities in the band at T = 296 K.

This situation is similar to that considered in Ref. 19, where for the $^{13}C^{16}O_2$ isotopic species we also found some bands absent from HITRAN. Figure 2 illustrates comparison of CDSD and HITRAN. The following value

$$100\% \cdot (I_{\mathrm{HITRAN}} - I_{\mathrm{CDSD}})/I_{\mathrm{CDSD}},$$

was used as a criterion for comparison of line intensities. Here I_{HITRAN} and I_{CDSD} are line intensities from HITRAN and CDSD taken at T = 296 K. One can see significant differences reaching 90%. We

believe that our modeling is more complete and accurate. Therefore, the data on $^{12}C^{16}O_2$ included in the HITRAN databank are to be updated.

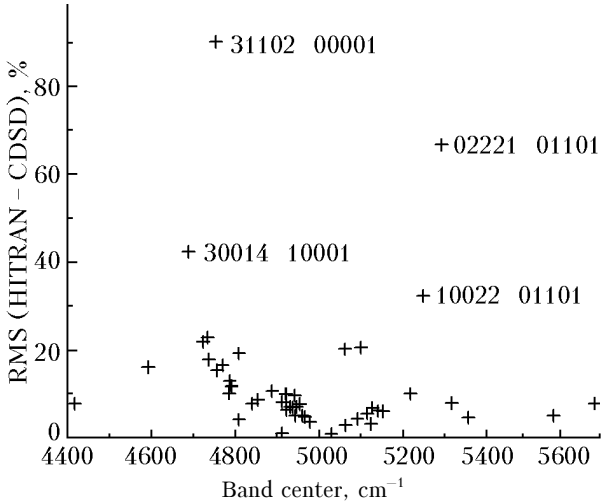

Fig. 2. Comparison of CDSD and HITRAN line intensities.

Acknowledgments

The author is glad to express his gratitude to Prof. V.I. Perevalov for useful discussion of the results presented in this paper.

References

1. J.B. Pollack, J.B. Dalton, D. Grinspoon, R.B. Wattson, R. Freedman, D. Crisp, D.A. Allen, B. Bezard, C. DeBergh, L.P. Giver, Q. Ma, and R. Tipping, Icarus **103**, 1–42 (1993).
2. R.M. Mihalcea, D.S. Baer, and R.K. Hanson, Appl. Opt. **37**, 8341–8347 (1998).
3. S.A. Tashkun, V.I. Perevalov, J.-L. Teffo, L.S. Rothman, and Vl.G. Tyuterev, J. Quant. Spectrosc. Radiat. Transfer **60**, 785–801 (1998).
4. S.A. Tashkun, V.I. Perevalov, J.-L. Teffo, and Vl.G. Tyuterev, J. Quant. Spectrosc. Radiat. Transfer **62**, 571–598 (1999).
5. K.P. Vasilevskii, L.E. Danilochkina, and V.A. Kazbanov, Opt. Spectrosc. **38**, 499–500 (1975).
6. F.P.J. Valero, C.B. Suarez, and R.W. Boese, J. Quant. Spectrosc. Radiat. Transfer **22**, 93–99 (1979).
7. F.P.J. Valero, C.B. Suarez, and R.W. Boese, J. Quant. Spectrosc. Radiat. Transfer **23**, 337–341 (1980).
8. C.B. Suarez and F.P.J. Valero, J. Mol. Spectrosc. **140**, 407–411 (1990).
9. L.P. Giver and Jr.C. Charkerian, J. Mol. Spectrosc. **148**, 80–85 (1991).
10. L.P. Giver, R.J. Kshirsagar, R.S. Freedman, R.B. Wattson, and L.R. Brown, in: *Proc. 5th Biennial HITRAN Conference* (Bedford, MA, 1998), p. 30.
11. R.B. Wattson, L.R. Giver, R.J. Kshirsagar, R.S. Freedman, and Jr.C. Charkerian, in: *Proc. 5th Biennial HITRAN Conference* (Bedford, MA, 1998), p. 29.
12. M. Fukabori, T.A. Aoki, T.E. Aoki, H. Ishida, and T. Watanabe, in: *Proc. 5th Biennial HITRAN Conference* (Bedford, MA, 1998), p. 32.
13. R.J. Kshirsagar, L.P. Giver, and Jr.C. Charkerian, J. Mol. Spectrosc. **199**, 230–235 (2000).
14. L.P. Giver, L.R. Brown, Jr.C. Charkerian, and R.S. Freedman, J. Quant. Spectrosc. Radiat. Transfer **78**, 417–436 (2003).
15. R.B. Wattson, private communication (1998).
16. L.S. Rothman, C.P. Rinsland, A. Goldman, S.T. Massie, D.P. Edwards, J.-M. Flaud, A. Perrin, C. Camy-Peyret, V. Dana, J.-Y. Mandin, J. Schroeder, A. McCann, R.R. Gamache, R.B. Wattson, K. Yoshino, K.V. Chance, K.W. Jucks, L.R. Brown, V. Nemtchinov, and P. Varanasi, J. Quant. Spectrosc. Radiat. Transfer **60**, 665–710 (1998).
17. S.A. Tashkun, V.I. Perevalov, J.-L. Teffo, A.D. Bykov, and N.N. Lavrentieva, J. Quant. Spectrosc. Radiat. Transfer (2003) (in print).
18. V.I. Perevalov, E.I. Lobodenko, O.M. Lulin, and J.-L. Teffo, J. Mol. Spectrosc. **171**, 435–452 (1995).
19. S.A. Tashkun, V.I. Perevalov, J.-L. Teffo, M. Lecoutre, T.R. Huet, A. Campargue, D. Bailly, and M.P. Esplin, J. Mol. Spectrosc. **200**, 162–176 (2000).